

# Full range analog Wheatstone bridge-based automatic circuit for differential capacitance sensors evaluation

G. Ferri, V. Stornelli, F. R. Parente, G. Barile

Authors are with the Department of Industrial and Information Engineering and Economic, University of L'Aquila, Italy;

Corresponding author: giuseppe.ferri@univaq.it

## SUMMARY

In this paper an integrable novel fully-analog Wheatstone bridge-based interface for differential capacitance estimation is presented. Its working principle takes advantage of the modified De-Sauty AC bridge configuration being employed only by two capacitors and two resistors. A feedback loop controls one of the resistors (e.g., a Voltage Controlled Resistor, VCR), to obtain an evaluation of the differential capacitance variation on a full range, thanks to a general but very simple formula which considers both the “autobalancing” and the bridge “out-of-equilibrium” ranges. The proposed interface shows a satisfactory accuracy, being the percentage relative error within 0.45% for the experimental results.

*KEYWORDS* — Differential capacitance sensors, bridge-based circuits, uncalibrated analog circuit, Wheatstone bridge

## 1. INTRODUCTION

At the present time there is a large demand of suitable low-cost systems (sensors and related electronics) for detecting environmental elements, for example physical displacement, pollutants or gas concentrations, also in reduced quantities, in different environments as safety and security [1]. Recent studies have also demonstrated that this issue is becoming important not only in special contexts (as industry and hospital), but also in everyday life (commercial places, schools, offices, houses, etc.) [2, 3].

Capacitive sensors can play an important role in this scenario: in fact they can directly measure physical-chemical parameters through the measurement of capacitive values variations.

A sub-set of these capacitive sensors is that formed by differential capacitive sensors, where the sensing element is represented by two capacitors with a common electrode: the capacitor relative values change in a complementary way under an external stimulus. In the literature, this kind of sensing is performed through different kinds of conversions: capacitance-to-frequency, capacitance-to-phase, capacitance-to-voltage (or current), etc. [4-7].

Concerning the impedance measurements, a classical solution is represented by the AC Wheatstone bridge. Bridge-based front-ends are usually utilized to estimate small resistive sensor variations by reading the output bridge voltage; in this sense, in the last years, many bridge-based interfaces have been exploited [8-15]. Automatic bridges consist of four impedances, connected in a suitable configuration where one impedance is the sensor, two impedances are fixed and the last one is variable. The unknown sensor impedance is obtained by balancing the bridge in “auto-tuning” configuration employing, as variable impedance, an automatic adjustable resistor or capacitor [16-19].

In this work, a novel interface for differential capacitive sensor is proposed. It is based on a capacitance-to-voltage conversion in continuous time developing a particular modified De-Sauty bridge (made up of two resistors and two capacitors as bridge elements), with a suitable feedback loop performing the auto-tuning of a Voltage Controlled Resistor (VCR). This autobalancing mechanism allows to know the unknown impedance value (i.e. the differential capacitive change) on a full range ( $\pm 100\%$ ) of variation.

The paper is organized as follows: in Section 2 a brief overview of differential capacitance sensors will be given, while the proposed bridge configuration and its theoretical calculations will be described in Section 3; in Section 4 the main significant simulation results will be presented and compared with measurements on a preliminary prototype board; finally, conclusions will be given in Section 5.

## 2. DIFFERENTIAL CAPACITANCE SENSORS: A BRIEF OVERVIEW

A differential capacitive sensor consists of two capacitors with a common plate, as shown in Fig. 1. The variations in the two series capacitances are of complementary kind.

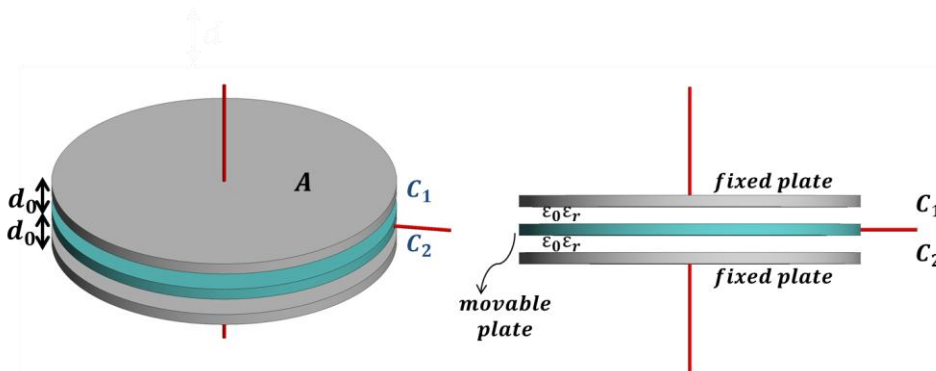


Fig. 1 : differential capacitance transducer.

Referring to Fig. 1 when the relative distance between an outer and the middle electrodes is changing linearly with  $x$ ,  $C_1$  and  $C_2$  have hyperbolic variations with  $x$ , as reported in (1), whereas if the areas of the capacitor plates is changing linearly with  $x$ ,  $C_1$  and  $C_2$  capacitances can be expressed according to (2) [20]:

$$C_{1,2} = \frac{C_0}{2} \frac{1}{(1 \mp x)} \quad , \quad (1)$$

$$C_{1,2} = \frac{C_0}{2} (1 \pm x) \quad , \quad (2)$$

being  $C_0$  the total capacitance of the transducer. The measurand  $x$  is independent from  $C_0$  value, being, in both the cases (1) and (2) and is equal to:

$$x = \frac{C_1 - C_2}{C_1 + C_2} \quad . \quad (3)$$

### 3. PROPOSED BRIDGE CONFIGURATION AND THEORETICAL CALCULATIONS

The proposed interface includes two basic electronic circuits, differential capacitive sensors and bridge-based front-ends, that are now merged in a single architecture in order to take advantage from both of them. In particular, the employment of a differential structure helps to reduce resolution problems related to common mode disturbs while the autobalancing of the VCR through a control voltage allows to extend the estimation range of the circuit.

This work shows a capacitance-to-voltage conversion employment in continuous time, by using a particular impedance bridge whose left branch is formed by the differential capacitive sensor ( $C_1, C_2$ ) and the right one by a fixed resistance ( $R$ ) and a Voltage Controlled Resistor (VCR, named  $R_{vcr}$ ) as shown in the block scheme in Figure 2. This VCR, in the autobalancing range, changes its value so balancing the bridge according to the relative capacitive variation. The choice in the placement of the components avoids the need of considering phase contribution in case of bridge unbalancing: this is also one of the main differences with respect to the previous published works (e.g., [19]) dealing with auto-balancing bridges and represents an easier and more versatile interface of differential or ratiometric transducers.

Due to VCR requirements about its input voltage ( $V_{ctrl}$  has to belong to  $[-10, 10]$  V range and should be a DC voltage), an integrator and a voltage divider ( $R_1, R_2$ ) before the VCR block have been included (see Fig. 2).

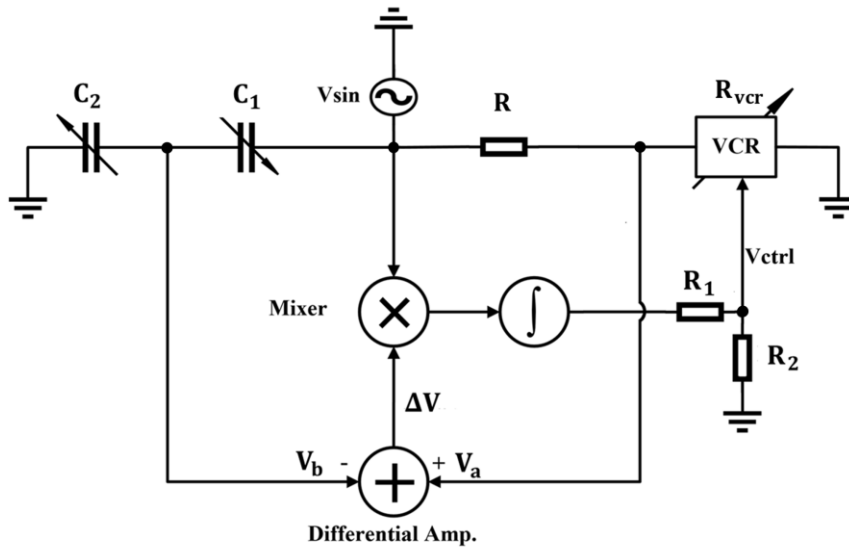


Fig. 2: block scheme of the proposed capacitive autobalancing bridge.

The electronic implementation of Figure 2 block scheme is shown in Figure 3. The  $R_{vcr}$  has been implemented by a commercial component AD633 [21] in a particular configuration (see further along the text); the same component, in a different configuration, constitutes the mixer block.

Differential capacitive variations change  $V_b$  value in the left branch of the bridge. As a consequence, through the feedback loop,  $V_{ctrl}$  level is varied and  $R_{vcr}$  changes its value so to force the bridge to be in equilibrium.

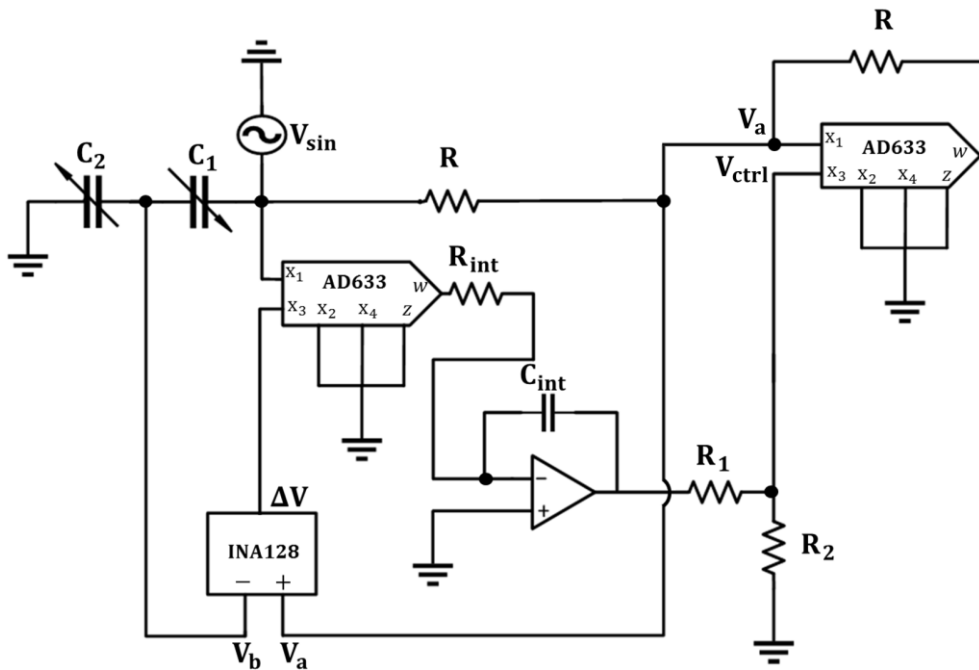


Fig. 3: electronic circuit of the proposed capacitive autobalancing bridge.

In this way it is possible to perform the accurate estimation of the measurand variable  $x$ , according to the following general formulations, valid for the full range of  $x$  variation ( $\pm 100\%$ ); in the two bridge branches we have respectively:

$$V_a = V_{\sin} \frac{R_{vcr}}{R + R_{vcr}}, \quad (4)$$

$$V_b = V_{\sin} \frac{\frac{1}{j\omega C_2}}{\frac{1}{j\omega C_1} + \frac{1}{j\omega C_2}} = V_{\sin} \frac{C_1}{C_1 + C_2}, \quad (5)$$

from which the bridge output difference is given by

$$V_a - V_b = \Delta V = V_{\sin} \left( \frac{R_{vcr}}{R + R_{vcr}} - \frac{C_1}{C_1 + C_2} \right). \quad (6)$$

Thus, with reference to (2):

$$C_1 = \frac{C_0}{2} + \Delta C = \frac{C_0}{2} (1 + x) \text{ where } x = \frac{2\Delta C}{C_0}, \quad (7)$$

$$C_2 = \frac{C_0}{2} - \Delta C = \frac{C_0}{2} (1 - x) \text{ where } x = \frac{2\Delta C}{C_0}, \quad (8)$$

being  $C_0$  the total differential sensor capacitance.

By rewriting (6) according to (7) and (8), it comes out that:

$$V_a - V_b = \Delta V = V_{\sin} \left( \frac{R_{vcr}}{R + R_{vcr}} - \frac{C_0(1+x)}{C_0(1+x) + C_0(1-x)} \right) = V_{\sin} \left( \frac{R_{vcr}}{R + R_{vcr}} - \frac{1+x}{2} \right). \quad (9)$$

Moreover, by considering the  $R_{vcr}$  implemented by the commercial components AD633, connected in a Zhong configuration as in Fig. 4 [21], the equivalent resistor is given by:

$$R_{vcr} = \frac{10R}{10 - V_{ctrl}}, \quad (10)$$

being the value “10” in the denominator expressed in Volt.

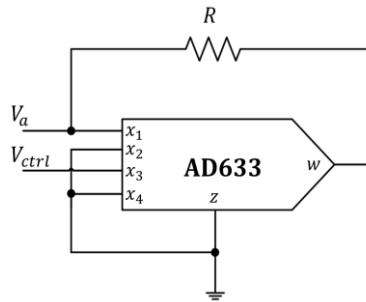


Fig. 4: Voltage Controlled Resistor implementation by means of the commercial components AD633.

Considering (9) and (10), we obtain:

$$\Delta V = V_a - V_b = V_{\sin} \left( \frac{\frac{10R}{10-V_{\text{ctrl}}} - \frac{1+x}{2}}{R + \frac{10R}{10-V_{\text{ctrl}}}} \right) = V_{\sin} \left( \frac{10}{20-V_{\text{ctrl}}} - \frac{1+x}{2} \right). \quad (11)$$

Manipulating (11), it is possible to write the following set of equations:

$$\frac{\Delta V}{V_{\sin}} (40 - 2V_{\text{ctrl}}) = 20 - (1+x)(20 - V_{\text{ctrl}}), \quad (12)$$

$$x(V_{\text{ctrl}} - 20) = \frac{\Delta V}{V_{\sin}} (40 - 2V_{\text{ctrl}}) - V_{\text{ctrl}}, \quad (13)$$

$$x = \frac{V_{\text{ctrl}} - \frac{\Delta V}{V_{\sin}} (40 - 2V_{\text{ctrl}})}{20 - V_{\text{ctrl}}}, \quad (14)$$

from which the relation for  $x$  is the following:

$$x = \frac{V_{\text{ctrl}}}{20 - V_{\text{ctrl}}} - 2 \frac{\Delta V}{V_{\sin}}. \quad (15)$$

In (15)  $V_{\text{ctrl}}$  is the voltage to be applied to the VCR, “20” is expressed in Volt,  $\Delta V$  is the differential amplifier output voltage (in terms of peak-to-peak level) and  $V_{\sin}$  is the supply sinusoidal voltage.

Eq. (15) reduces to the following very simple relation:

$$x = \frac{V_{\text{ctrl}}}{20 - V_{\text{ctrl}}}, \quad (16)$$

in the case of bridge in equilibrium ( $\Delta V=0$ ).

#### 4. THEORETICAL vs MEASURED AND SIMULATED RESULTS

The following values have been considered for this case-study:  $R= 33 \text{ k}\Omega$ ,  $R_1=2.7 \text{ k}\Omega$ ,  $R_2=5.6 \text{ k}\Omega$ ,  $R_{\text{int}} = 200 \text{ k}\Omega$  and  $C_{\text{int}}=20 \text{ pF}$ . Concerning the choice of  $C_0$ , it is possible to consider values as low as  $10 \text{ pF}$ , but in measurements we have chosen a baseline of  $C_1 = C_2 = C_0/2 = 200 \text{ pF}$ , so to certainly neglect other capacitive parasitic effects.

The measurand  $x$  is determined by reading two values:  $V_{\text{ctrl}}$  in the autobalancing range (where the bridge is in equilibrium and  $\Delta V=0$ ) and  $\Delta V$  in “out-of-range” (where  $V_{\text{ctrl}}$  is at saturation value  $\pm 9.65 \text{ V}$  and  $\Delta V$  is not zero). Eq.(15) is a general expression for evaluating the capacitive variation in the whole capacitance range ( $\pm 100\%$ ), as shown in Fig. 5. In the autobalancing range it is possible to use (16) to determine  $x$  through the reading of only  $V_{\text{ctrl}}$  value.

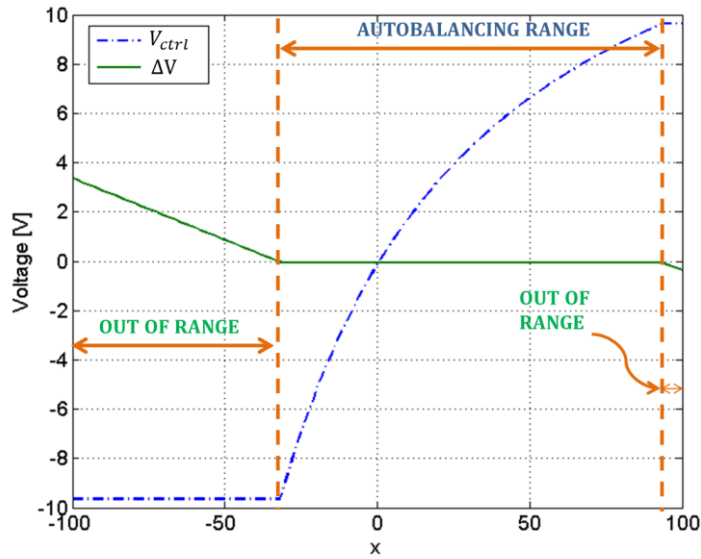


Fig. 5:  $V_{ctrl}$  and  $\Delta V$  behaviours vs  $x$ : simulated results.

The absolute error (defined as in [22]) between theory and simulation vs.  $x$  is shown in Fig. 6. Its absolute value is lower than 0.07 V in the worst case.

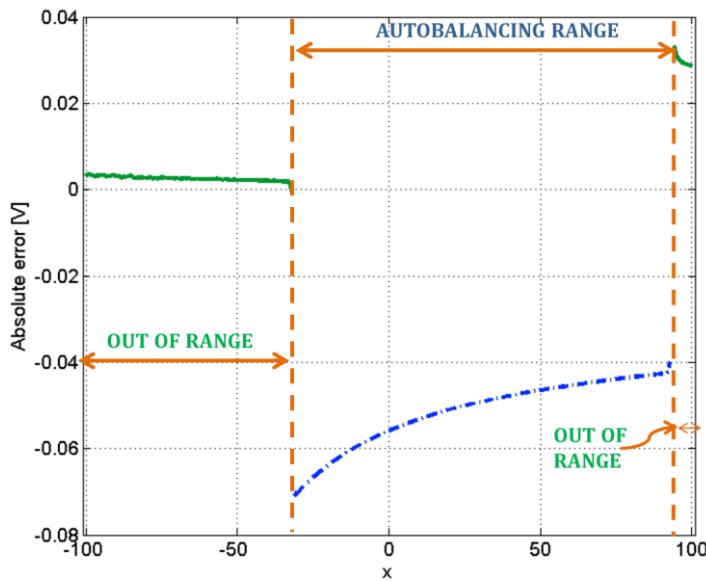


Fig. 6: absolute error in “autobalancing” interval and “out-of-range” vs.  $x\%$ : theoretical vs. simulated results.

It is important to underline that simulation results in Figs. 5-6 are completely independent from the baseline value if  $C_0 > 10$  pF.

Experimental tests have been conducted on a discrete element board, demonstrating the circuit capability to follow the capacitive sensor variations in a full estimation range, as shown in Fig. 7. In fact, the percentage relative error, defined as in [22], is lower than 0.45 %, as visible in Fig. 8.

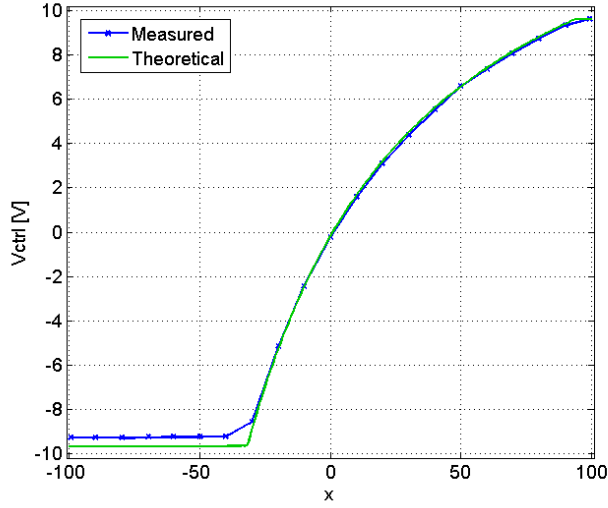


Fig. 7:  $V_{ctrl}$  behaviour vs  $x$ : theoretical and experimental results.

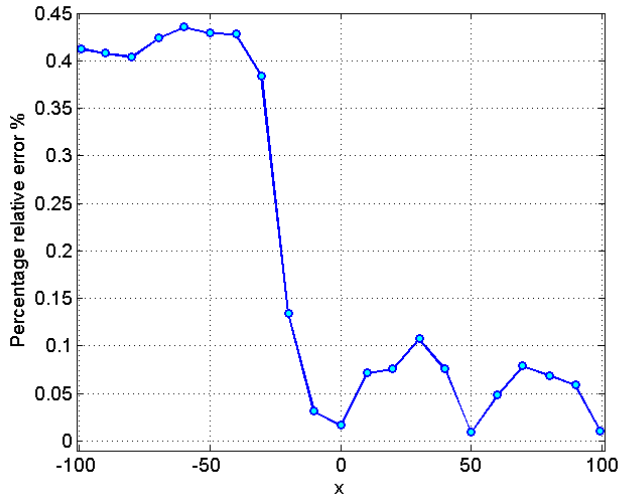


Fig. 8: percentage relative error vs.  $x$ : theoretical vs. experimental results.

A comparison of the interface results, with respect to other solutions reported in the literature, is presented in Table I. The proposed circuit shows a good accuracy with respect to other approaches.

TABLE I  
COMPARISON TABLE

Ref.	[4]	[5]	[6]	[7]	[11]	[13]	[14]	This work
Capacitance value[F]	20 p ( $\pm 120\%$ )	0.9 p ( $\pm 100\%$ )	500 p ( $\pm 50\%$ )	400 p ( $\pm 50\%$ )	200-1200 p	n.a.	25-840 n ( $\pm 100\%$ )	400 p ( $\pm 100\%$ )
Approach	C to V	C to I	C to V	C to T	C to V	C to V	C to V	C to V
Circuit topology	Discrete	Integrated	Discrete	Discrete	Discrete	Discrete	Discrete	Discrete
Accuracy (error)	1.5 mV	< 1.5%	$\pm 0.03\%$	0.9%	< 6%	10 $\mu$ V	< 10%	< 0.45%

## 5. CONCLUSIONS

In this paper the authors have presented a novel automatic bridge-based interface performing differential capacitive sensor measurements on a full range De-Sauty AC bridge topology. Simulated and experimental results have confirmed the theoretical expectations which allow the capacitance estimation in its the full variations range with a good accuracy, making the proposed interface solution suitable for several application.

## REFERENCES

1. Katic, N., Kazi, I., Tajalli, A., Schmid, A., Leblebici, Y., A subthreshold current-sensing  $\Sigma\Delta$  modulator for low-voltage and low-power sensor interfaces, *International Journal of Circuit Theory and Applications* **2015**; **43(11)**, pp. 1597-1614.
2. De Jong, C., Meijer, G. C. M., A high-temperature electronic system for pressure transducers, *IEEE Transactions on Instrumentation and Measurement* **2000**; **49**, pp. 365–370, DOI: 10.1109/19.843079.
3. D'Amico, A., Di Natale, C., Falconi, C., Martinelli, E., Paolesse, R., Pennazza, G., Santonico, Detection and identification of cancers by the electronic nose, *Expert Opinion on Medical Diagnostics* **2012**; **356(6)**, pp. 175–185.
4. Mochizuki, K., Watanabe K., Masuda, T., A High-Accuracy High-Speed Signal Processing Circuit of Differential-Capacitance Transducers, *IEEE Trans. on Instrumentation and Measurement* **1998**; **47**, pp. 1244-1247.
5. Scotti, G., Pennisi, S., Monsurrò, P., Trifiletti, A., 88- $\mu$ A 1-MHz Stray-Insensitive CMOS Current-Mode Interface IC for Differential Capacitive Sensors, *IEEE Transactions on Circuits and Systems I: Regular Papers* **2014**; **61(7)**, pp. 1905-1916.
6. George, B., Kumar, V. J., Switched capacitor signal conditioning for differential capacitive sensors, *IEEE Trans. on Instrumentation and Measurement*, **2007**; **56**, pp. 913-917.
7. Mohan, N. M. , Shet, A. R. , Kedarnath, S. , Kumar, V. J., Digital converter for differential capacitive sensors, *IEEE Trans. Instrum. Meas* **2008**; **57**, pp. 2576–2581.
8. Dutta, M., Rakshit, A., Bhattacharyya, S. N. , Development and study of an automatic AC bridge for impedance measurement. *IEEE Transactions on Instrumentation and Measurement*, **2001**; **50(5)**, pp. 1048-1052.
9. Jordana, J., Pallas-Areny, R., A simple efficient interface circuit for piezo-resistive pressure sensors, *Sensors and Actuators A* **2006**; **127**, pp. 69–73.
10. Zhang, J. , Zhang, K., Wang, Z., Mason, A., A universal micro-sensor interface chip with network communication bus and highly programmable sensor readout, in: *The 2002 45th Midwest Symposium on Circuits and Systems*, **2002**; **361**, pp. 246–249.
11. Lopez-Martin, A.J., Zuza, M., Carlosena, A. , A CMOS interface for resistive bridge transducers, *IEEE International Symposium on Circuits and Systems ISCAS*, **2002**; **391** , pp. 153–156.
12. Malik, S., Kishore, K., Islam, T., Zargar, Z. H., Akbar, S. A., A time domain bridge-based impedance measurement technique for wide-range lossy capacitive sensors, *Sensors and Actuators A: Physical*, **2015**; **234**, pp. 248-262.
13. Ferrari, V., Ghisla, A., Vajna, Z. K., Marioli, D., Taroni, A., ASIC front-end interface with frequency and duty cycle output for resistive-bridge sensors. *Sensors and Actuators A: Physical*, **2007**; **138(1)**, pp. 112-119
14. Van der Goes, F.M.L. , Meijer, G.C.M. , A simple accurate bridge-transducer interface with continuous autocalibration, *IEEE Transactions on Instrumentation and Measurement*, **1997**; **46**, pp. 704–710.
15. Aaltonen, L., Rahikkala, P., Saukoski, M., Halonen, K., High-resolution continuous-time interface for micromachined capacitive accelerometer, *International Journal of Circuit Theory and Applications* **2009**, **37(2)**, pp. 333-349.
16. De Marcellis, A., Ferri, G., Mantenuto, P., A novel 6-decades fully-analog uncalibrated Wheatstone bridge-based resistive sensor interface, *Sensors and Actuators B: Chemical*, **2013**; **189**, pp. 130-140.
17. De Marcellis, A., Ferri, G., Mantenuto, P., Analog Wheatstone bridge-based automatic interface for grounded and floating wide-range resistive sensors, *Sensors and Actuators B: Chemical*, **2013**; **187**, pp. 371-378.

18. Mantenuto, P., Ferri, G., De Marcellis, A., Uncalibrated automatic bridge-based CMOS integrated interfaces for wide-range resistive sensors portable applications, *Microelectronics Journal*, **2014**; **45(6)**, pp. 589-596.
19. Mantenuto P., De Marcellis A., Ferri G., “Novel Modified De-Sauty Autobalancing Bridge-Based Analog Interfaces for Wide-Range Capacitive Sensor Applications”, *IEEE Sensors Journal*, **2014**; **14(5)**, pp.1664-1672.
20. Ferri, G. Parente, F.R., Stornelli, V., Analog current-mode interfaces for differential capacitance sensing, Proc. of IEEE Sensors Applications Symposium (SAS), Catania, April **2016**.
21. Analog Devices, Norwood, MA, USA. Datasheet, AD633, Low Cost Analog Multiplier. [Online]. Available: [www.analog.com/media/en/technical/data-sheets/AD633.pdf](http://www.analog.com/media/en/technical/data-sheets/AD633.pdf), **2011**.
22. D'Amico, A., Di Natale, C., A contribution on some basic definitions of sensors properties, *IEEE Sensors Journal*, **2001**; pp. 183–190.